JOURNAL OF GEOPHYSICAL RESEARCH, VOL. 104, NO. D1, PAGES 1705–1715, JANUARY 20, 1999

Sources of upper tropospheric HO_X: A three-dimensional study

Jean-François Müller

Belgian Institute for Space Aeronomy, Brussels

Guy Brasseur

National Center for Atmospheric Research, Boulder, Colorado

Abstract. The sources of odd hydrogen radicals (HO_x=OH+HO_2) in the upper troposphere are investigated and quantified using a three-dimensional model. While the reaction of $O(^1D)$ with water vapor constitutes the single major source of HO_x in the lower and middle troposphere, the model calculations suggest that acetone photooxidation represents a large, almost ubiquitous source of HO_x in the upper troposphere (around 20-40% of the total primary source in the main aircraft corridors, poleward of 40°N), while the convective injections of peroxides and aldehydes are the dominant sources in the tropics, above the oceans and the continents, respectively. The consequences for ozone photochemical production in the upper troposphere are discussed, in particular, in the perspective of the aircraft impact. The role of acetone on ozone photochemical production is estimated and discussed. It is calculated that the presence of acetone might enhance by about 20% the sensitivity of upper tropospheric ozone to the current aircraft emissions of NO_x.

1. Introduction

The supply of hydrogen radicals (HO_x=OH+HO_2) is known to be an important factor controlling the photochemical production of ozone in the troposphere. In particular, quantifying the additional production of ozone caused by a particular source of nitrogen oxides (NO_x), such as the subsonic aircraft fleet, requires that the different sources and sinks of HO_x be appropriately described in chemistry-transport models. It has been suggested [e.g., *Wennberg et al.*, 1998] on the basis of recent in situ measurements that upper tropospheric HO_x levels are often substantially higher than those predicted using "classical" models, i.e., when the only sources of HO_x are the $O(^1D)$+H_2O reaction and the photolysis of (methane-derived) formaldehyde. The photolysis of acetone and the convective injection (followed by photolysis) of lower tropospheric peroxides and possibly carbonyls have been invoked in order to resolve the discrepancy. In that perspective the question arises of whether the published estimates of the subsonic aircraft impact on ozone [e.g., *Brasseur et al.*, 1996; *Friedl*, 1997] should be revised and by how much. While recent studies [e.g., *Wennberg et al.*, 1998; *Jaeglé et al.*, 1997; *Folkins et al.*, 1997, 1998] give useful insights as to the importance of particular sources of HO_x at the local level (i.e., at the times and locations of the observations), there is still a need for a more global view of the upper tropospheric HO_x sources.

The present study attempts to determine the relative importance of the different sources of HO_x in the upper troposphere, using a global chemistry-transport model, the Intermediate Model for the Global Evolution of Species (IMAGES) model. An important rationale for this study is to allow for a better estimate of the aircraft impact and its uncertainties. The relative importance of the HO_x sources with respect to ozone production will be discussed on the basis of the model results. This model will be briefly described in section 2. In addition, comparisons with observations will be presented for the most relevant species, in order to give some insights on the model performance. The methodology used for the determination of the HO_x sources will be discussed in section 3. The results for HO_x and O_3 production will be presented and discussed in sections 4 and 5, respectively.

Paper number 1998JD100005.
0148-0227/99/1998JD100005$09.00

2. Model Description and Validation

The major features of the IMAGES model have been described by *Müller and Brasseur* [1995]. This three-dimensional chemical transport model calculates the distribution of about 60 species, including O_3, HO_x, NO_x, sulfur oxides, methane, nonmethane hydrocarbons (ethane, ethylene, propylene, isoprene, α-pinene, and n-butane as a surrogate for the other higher hydrocarbons, also propane and acetone; see below), and their degradation products. Its horizontal resolution is 5° in latitude and in longitude. In the vertical the model includes 25 σ layers extending from the Earth's surface to the lower stratosphere (50 mbar). Large-scale transport is driven by monthly averaged winds taken from an analysis of the European Centre for Medium-Range Weather Forecasts (ECMWF). The impact of wind variability at timescales smaller than one month is taken into account as a diffusion process, with diffusion coefficients estimated from the ECMWF wind variances. The water vapor distribution is also provided by the ECMWF analysis. Vertical mixing in the planetary boundary layer is also represented as diffusion. The effect of deep convection on vertical transport is parameterized following the scheme of *Costen et al.* [1988]. The distribution of cloud updrafts is parameterized using the Cumulo-nimbus distribution estimated by the International Satellite Cloud Climatology Project (ISCCP) ("D2" climatology).

In the most recent version of the model, convection and wet scavenging schemes are modified for the very soluble species (HNO_3, H_2O_2, and sulfates) in order to account more consistently for the effect of rainout in the convective updrafts. While the downdraft velocity is identical for soluble and unsoluble species, the updraft intensity is scaled by a factor $1 - p_{efl}$, where p_{efl} is the precipitation efficiency (defined as the ratio of precipitation to the

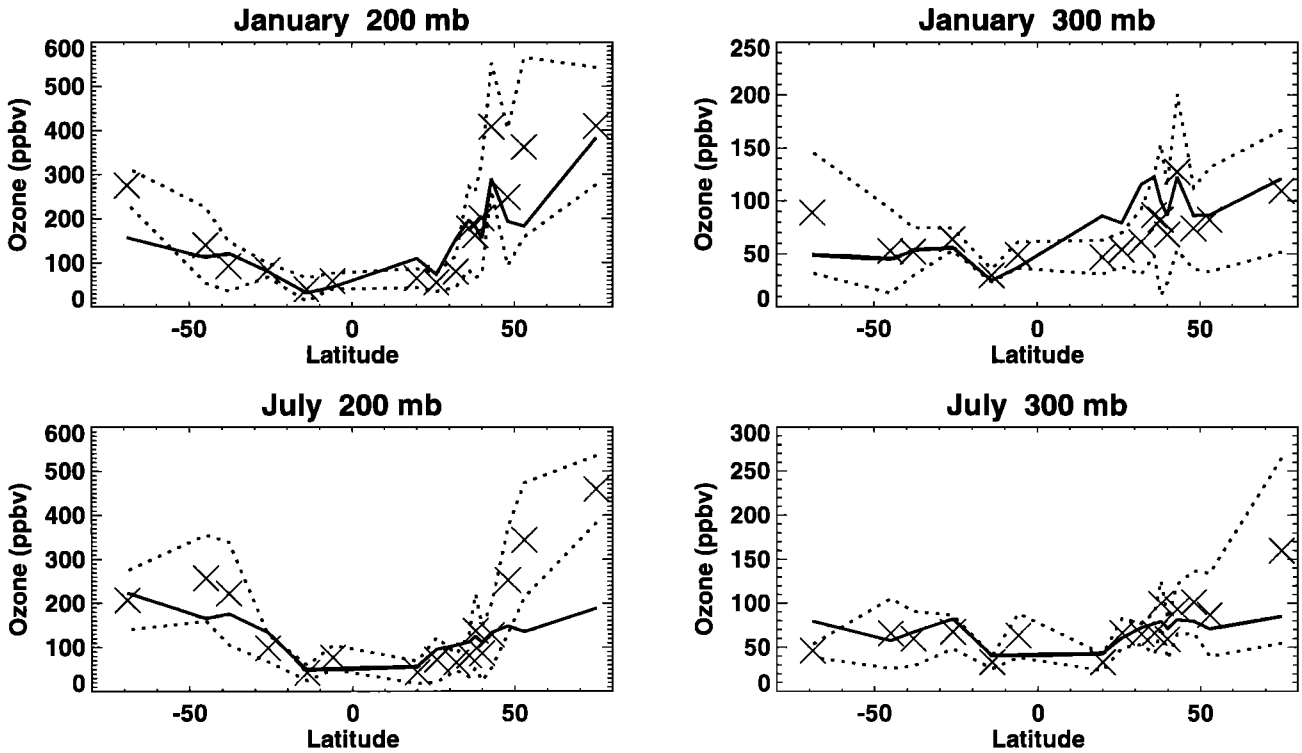

Figure 1. Observed (crosses are monthly means; and dotted lines are ± one standard deviations) and modeled (solid line) ozone mixing ratios (ppbv) at 200 and 300 mbar, in January and July. Observations are from ozone soundings compiled by J. A. Logan (manuscript in preparation, 1998). The sounding locations are, from north to south: Resolute (75°N), Edmonton (53°N), Hohenpeissenberg (48°N), Sapporo (43°N), Boulder (40°N), Wallops Island (38°N), Tateno (36°N), Kagoshima (32°N), Naha (26°N), Hilo (20°N), Natal (6°S), Samoa (14°S), Pretoria (26°S), Aspendale/Laverton (38°S), Lauder (45°S), and Syowa (69°S).

total water vapor inflow), parameterized according to *Fritsch and Chappell* [1980] as a function of the vertical wind shear between cloud base and cloud top. The remaining fraction of the convective updraft flux is rained out. It is therefore assumed that the very soluble gases are entirely in the condensed phase in the updraft. The calculated precipitation efficiency (taken to be 100% in, for example, the Harvard [*Balkanski et al.*, 1993] and Model of the Global Universal Tracer Transport In the Atmosphere (MOGUNTIA) models [e.g., *Dentener and Crutzen*, 1994]) is often close to 90% in tropical regions and takes lower values at midlatitudes, typically 30% or less in areas where the jet stream is strongest. In spite of these model improvements, we acknowledge that the treatment of washout and convection in a monthly-mean model such as IMAGES is relatively crude and might be a source of bias in the model results.

The trace gas emissions used in the model are those of *Müller and Brasseur* [1995], except that the Global Emissions Inventory Activity (GEIA) inventories are now used for the fossil fuel emissions of NO_x and SO_x [*Benkovitz et al.*, 1996] as well as for the biogenic continental emissions of nonmethane hydrocarbons (NMHC) [*Guenther et al.*, 1995] and NO_x [*Yienger and Levy*, 1995]. The lightning source of NO is distributed following *Price et al.* [1997] in the horizontal and following *Pickering et al.* [1998] in the vertical. It is scaled to a global source of 3 TgN yr^{-1}. The biomass burning emissions used are described by *Granier et al.* [1996], except for the NO_x emissions, where the emission ratios relative to CO_2 are assumed to be 0.28% for savanna burning [*Andreae et al.*, 1996] and 0.15% for fuelwood burning [*Brocard et al.* 1998], resulting in a global annual source of 8 TgN yr^{-1}.

The chemistry of propane and acetone has been added to the model. The chemical mechanism and rate constants are taken from *Kanakidou et al.* [1991], with updates from *De More et al.* [1997] and *Jenkin et al.* [1997]. The new species considered in the mechanism are C_3H_8, $C_3H_8O_2$, and C_3H_8OOH (surrogates for two isomers) and acetone, $CH_3COCH_2O_2$, CH_3COCH_2OOH, and CH_3COCH_2O. The formation of propionaldehyde is neglected, since it is a minor route for propane oxidation. The photolysis cross sections and quantum yield for acetone are taken from T. Gierczak et al. (Photochemistry of acetone under tropospheric conditions, submitted to *Chemical Physics*, 1997) and *McKeen et al.* [1997]. Propane emissions include fossil fuel burning and natural gas exploitation (totaling 11 Tg yr^{-1}), biomass burning (3 Tg yr^{-1}), the ocean (1 Tg yr^{-1}), and a biogenic source (2 Tg yr^{-1}). Acetone emissions include fossil fuel burning (1 Tg yr^{-1}), biomass burning (16 Tg yr^{-1}, the emission ratio being a fraction of the total nonmethane hydrocarbons (NMHC) emissions from *Granier et al.* [1996]), and vegetation (23 Tg yr^{-1}, distributed as the isoprene and terpenes emissions, in equal proportions). The total biogenic source has been adjusted in order to provide a good agreement between the model results and aircraft observations in tropical regions (see validation below). This biogenic source should be regarded as a sum of a direct biogenic source and an indirect production from the oxidation of higher biogenic hydrocarbons, for example, terpenes and methyl-butenol. The production of acetone from the oxidation of propane and higher alkanes

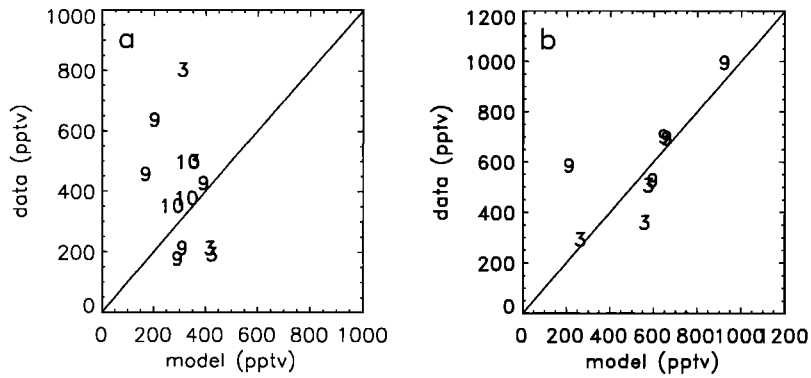

Figure 2. Observed versus modeled mixing ratios of (a) H_2O_2 and (b) acetone, at or around 300 mbar. The numbers denote the measurements campaign: 3, March, Pacific Exploratory Mission West-B (PEM-West-B) (South Asia Coast, West Pacific, and West Equatorial Pacific), 9, September, Transport and Atmospheric Chemistry Near the Equator-Atlantic (TRACE A) (East Brazil, South Brazil, Ascension, West Africa Coast, and South Africa), 10, October, PEM-West A (East China Sea, Japan Coast, and Tropical West Pacific). Compilations of observations are as those by *Wang et al.* [1998b] and *Hauglustaine et al.* [1998].

(represented by n-butane in the model) amounts to 18 and 9 Tg yr^{-1}, respectively.

The IMAGES model results, as well as comparisons with observations, have been presented by, for example, *Müller and Brasseur* [1995] and *Friedl* [1997]. However, in order to ascertain the robustness of the results presented in sections 3-5, some additional model validation focusing on the species of interest for the upper tropospheric HO_x budget is given here. The calculated monthly averaged ozone mixing ratios at 200 and 300 mbar are compared to ozonesonde measurements in Figure 1. It is seen that the model reproduces the main features of the observed ozone distribution, although noticeable discrepancies are apparent. The model tends to underestimate ozone at 200 mbar at high latitudes and to overestimate ozone in the 20°-35°N latitude band. In both cases, possible model transport flaws are most likely to cause the disagreement. In July, however, there is a fairly good agreement between the model and the observations at all tropospheric latitudes.

A comparison for upper tropospheric (300 mbar) H_2O_2 and acetone concentrations corresponding to selected (mostly tropical) aircraft campaigns is displayed in Figure 2. The discrepancies are generally larger for H_2O_2, partly because of its short photochemical lifetime and hence its large variability that cannot be reproduced by the model using monthly averaged dynamical and cloud fields. Figure 2 suggests that the modeled H_2O_2 might generally be too low in these regions, possibly because convective injection of H_2O_2 from the lower troposphere is underestimated. In some cases, however (e.g. the South Brazil area in the Transport and Atmospheric Chemistry Near the Equatorial Atlantic (TRACE A) campaign), H_2O_2 is underestimated by the model at all altitudes, indicating that other processes might not be well represented. Possible differences between the water vapor fields in the model and those during the observations might be an important cause of discrepancies for H_2O_2. For acetone the good agreement displayed in Figure 2 suggests that the adopted large biogenic and biomass burning emissions are realistic, even though the exact nature of the biogenic source is not elucidated. Similar conclusions were drawn by *Wang et al.* [1998a] using the Harvard model. We calculate that using the acetone-CO correlation proposed by *McKeen et al.* [1997] on the basis of the Pacific

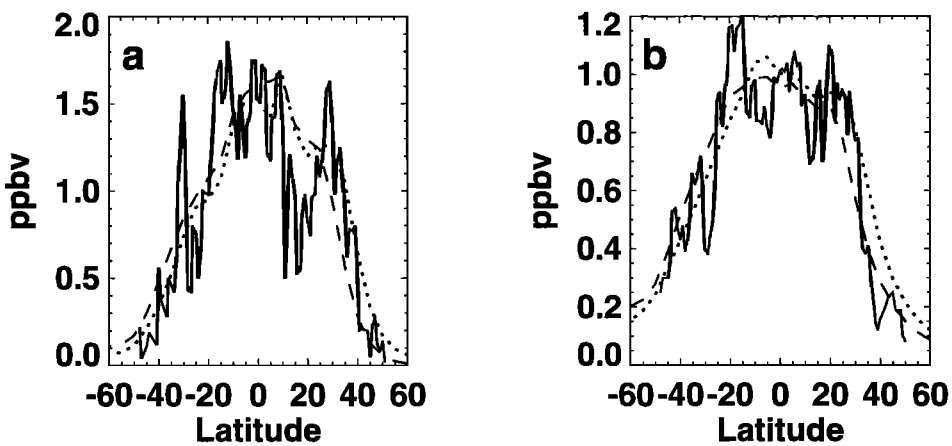

Figure 3. Observed (solid line) and modeled (dotted line for October and dashed line for November) mixing ratios of (a) H_2O_2 and (b) organic peroxides (ROOH), both in parts per billion by volume. Observations are the ship measurements of the R/V *Polarstern* across the Atlantic Ocean (October 20 to November 12, 1990) [*Slemr and Tremmel*, 1994]. Model results are for 30°W.

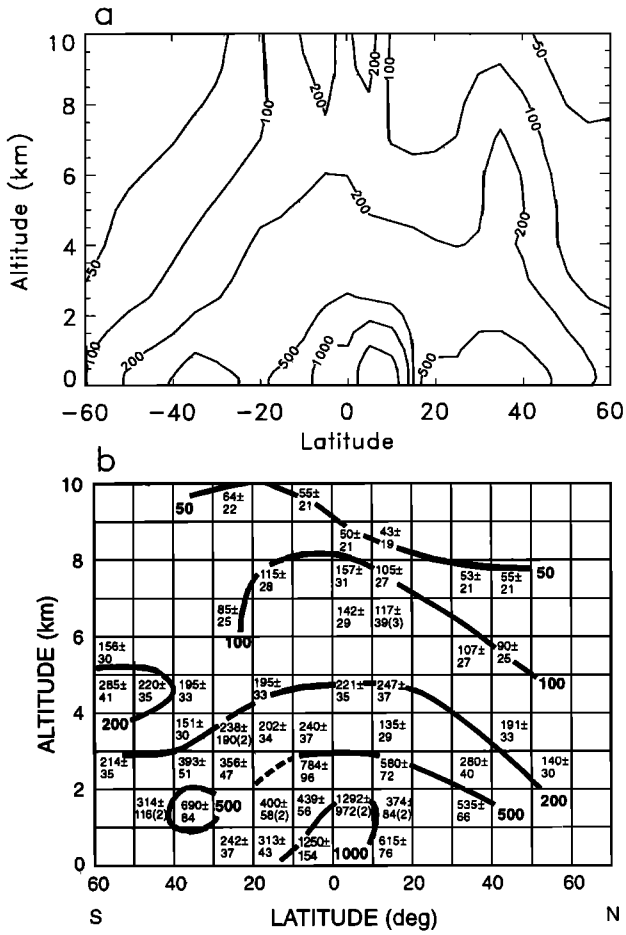

Figure 4. (a) Modeled and (b) observed mixing ratios of CH_2O, in parts per trillion by volume. Observations are the aircraft measurements of the southbound TROPOZ II campaign flights [*Arlander et al.*, 1995].

Exploratory Mission-West B (PEM-West B) result would result in a better agreement between the model and the observations for the PEM-West B observations but in an underestimate (20-30%) for the TRACE A results. Additional measurements, improved biogenic emission inventories, and biogenic NMHC degradation schemes will be needed to refine the global acetone budget.

In Figure 3 the modeled peroxides' (H_2O_2 and organic ROOHs) concentrations at 30°W (surface level) are compared with ship measurements (R/V *Polarstern* in 1990) over the Atlantic Ocean [*Slemr and Tremmel*, 1994]. In both cases a good agreement is noted. The H_2O_2 overestimate around 20°N might be due to an underestimation of the dry deposition in this region [*Slemr and Tremmel*, 1994]. Note that the calculated ROOH concentration consists mostly (>90%) of methyl hydroperoxide (CH_3OOH) over oceanic areas.

Finally, Figures 4a and 4b display a comparison of the modeled and observed CH_2O concentrations in January along the southbound flights of the Tropospheric Ozone (TROPOZ) II campaign [*Arlander et al.*, 1995]. In both the measurements and the model results, the largest concentrations (>1 ppbv) are found in the boundary layer around the equator, i.e., over tropical South America, while values generally lower than 200 pptv are found above 4 km altitude. The modeled concentrations are, however, higher than those observed in the upper troposphere near the equator as well as around 35°N. Our analysis indicates that these high values are caused by convective transport of formaldehyde precursors (e.g., isoprene). The coarse resolution of the model makes it difficult to reproduce the strong concentration gradient between the Pacific Ocean and South America; the TROPOZ II samples in the upper troposphere are most likely to be of maritime origin in these regions. At 35°N, the unrealistic peak is due to the high convective activity near the Atlantic Coast of the United States in the model.

3. Calculating the HO_x Sources

It is well known that the single largest source of HO_x in most of the troposphere is provided by photolysis of ozone and the subsequent reaction of $O(^1D)$ with water vapor [*Levy*, 1972]:

$$O_3 + h\nu \rightarrow O_2 + O(^1D) \quad (1)$$
$$O(^1D) + H_2O \rightarrow 2\,OH \quad (2)$$

This is the major mechanism responsible for the oxidizing capacity of the troposphere as a whole. It is especially effective in the lower troposphere in tropical regions and in the summer midlatitudes, where water vapor as well as UVB radiation are abundant. In the upper troposphere, however, where water vapor mixing ratios are very low and where ozone is still much less abundant than in the stratosphere, other sources have been proposed that could be significant or even dominant under certain conditions. The proposed sources include the oxidation of methane in the presence of NO_x [e.g., *Logan et al.*, 1981], the photolysis of acetone [*Singh et al.*, 1995; *McKeen et al.*, 1997], and the convective injection of lower tropospheric peroxides and formaldehyde, followed by their photolysis in the upper troposphere [*Wennberg et al.*, 1998; *Jaeglé et al.*, 1997; *Prather and Jacob*, 1997; *Arnold et al.*, 1997; *Chatfield and Crutzen*, 1984]. The significance of these processes on the global scale, however, is still debated and remains unclear.

Before investigating the role of these sources in more detail, it is important to define the primary and secondary sources of HO_x and to distinguish between them in the following discussion. Primary sources are provided by photochemical reactions that do not necessarily involve the presence of OH or HO_2. An example of a primary source is provided by (1) and (2). The secondary sources are those that require the presence of HO_x to operate and that increase linearly, or almost linearly, with the abundance of HO_x. These sources therefore amplify the production of HO_x by the primary sources. An important example of a secondary source is the oxidation of methane by OH in the presence of NO_x. This source is dependent on the local photochemical conditions that determine the fate of the short-lived intermediates of the methane oxidation through the following reactions:

$$CH_3O_2 + NO\ (+O_2) \rightarrow CH_2O + HO_2 + NO_2 \quad (3)$$
$$CH_3O_2 + HO_2 \rightarrow CH_3OOH + O_2 \quad (4)$$
$$CH_3OOH + OH \rightarrow CH_3O_2 + H_2O \quad (5)$$
$$CH_3OOH + OH \rightarrow CH_2O + OH + H_2O \quad (6)$$
$$CH_3OOH + h\nu\ (+O_2) \rightarrow CH_2O + HO_2 + OH \quad (7)$$
$$CH_2O + h\nu\ (+O_2) \rightarrow CO + 2\,HO_2 \quad (8)$$
$$CH_2O + h\nu \rightarrow CO + H_2 \quad (9)$$
$$CH_2O + OH\ (+O_2) \rightarrow CO + HO_2 + H_2O \quad (10)$$

In the high-NO_x limit, (4)-(7) can be neglected, and a net HO_x production results from the photolysis of formaldehyde (reaction (8)). Under these conditions the HO_x yield resulting from the

CH_4+OH reaction is equal to about 0.6 (HO_x molecules produced per molecule of CH_4 oxidized). Under realistic conditions, however, the consumption of OH and HO_2 by (4) and (5) results in lower values of the net yield. According to our model, these values range most frequently between 0.3 and 0.6 in the upper troposphere, except in the very low NO_x regions of the equatorial Pacific, where lower, sometimes negative yields are predicted. These values were estimated by assuming photochemical equilibrium for the chemical intermediates, using the oxidant (OH, HO_2, NO, and light) concentrations predicted by the IMAGES model.

The almost linear dependence of this net HO_x production on the atmospheric abundance of HO_x is due to the long lifetime of methane, implying that the local methane concentration is almost unaffected by the OH levels in the upper troposphere. To some extent, this is also true for ethane (C_2H_6), since its lifetime of about two months is longer than the timescale for transport between the upper and lower parts of the troposphere (a few weeks). The net HO_x yields resulting from C_2H_6+OH and CH_4+OH are estimated here to be similar on a per molecule basis. The impact of ethane, however, is minor because of its low abundance in the troposphere.

In contrast with the oxidation of methane and ethane, the photooxidation in the upper troposphere of much shorter-lived species injected from the lower troposphere should be considered as a primary source of HO_x. This applies to the injection of peroxides, aldehydes, and even species like isoprene and the terpenes. These compounds have lifetimes of the order of 1 day or less and are almost entirely oxidized in the upper troposphere whenever they are transported to these altitudes. The peroxides as well as the aldehydes are oxidized by either photolysis or reaction with OH, and the yield of HO_x resulting from their oxidation generally decreases with increasing HO_x concentrations, because photolysis usually leads to higher net HO_x production than that of the reaction with OH. In the case of formaldehyde and hydrogen peroxide (H_2O_2), photolysis is the only HO_x source. For most other species the OH reaction leads to a net HO_x production, whose magnitude depends on the photochemical conditions. For example, acetaldehyde is oxidized through the following reactions:

$$CH_3CHO + OH\ (+O_2) \rightarrow CH_3CO_3 + H_2O \quad (11)$$
$$CH_3CO_3 + NO \rightarrow CH_3O_2 + NO_2 \quad (12)$$
$$CH_3CO_3 + NO_2 + M \rightarrow PAN + M \quad (13)$$
$$PAN + h\nu \rightarrow CH_3CO_3 + NO_2 \quad (14)$$
$$PAN + M \rightarrow CH_3CO_3 + NO_2 + M \quad (15)$$

followed by (3)-(10). Owing to the long lifetime of peroxyacetylnitrate (PAN) in the upper troposphere (a few weeks), some of the PAN formed through (13) is transported down and is decomposed in the lower troposphere, so that this reaction is a radical sink in the upper troposphere. In spite of that, the OH oxidation of acetaldehyde results in a net production of HO_x similar to that of CH_4+OH on a per molecule basis. Comparable HO_x yields are calculated for the OH-oxidation of CH_3OOH and glycolaldehyde $CH_2(OH)CHO$. The complexity of higher hydrocarbon oxidation schemes makes it very difficult to extend these calculations to all nonmethane hydrocarbons in a systematic way. Furthermore, many important kinetic processes and rates involved in the chemistry of higher NMHC are still very uncertain, and global models such as IMAGES make use of simplified reaction mechanisms whose validity needs to be checked with respect to net HO_x formation.

For these reasons and for the sake of simplicity, we will restrict our discussion and results to the injection of the peroxides H_2O_2 and CH_3OOH and the aldehydes CH_2O, CH_3CHO, and CH_2OHCHO. For the C_2 aldehydes we calculate also the effect of their production in the upper troposphere from the oxidation of precursors NMHC (isoprene, α-pinene, the C_2-C_3 alkenes, and the surrogate n-butane [*Müller and Brasseur*, 1995]). In order to estimate the impact of transport from the lower troposphere on the concentrations of these species in the upper troposphere, we include in the model fictitious chemical species (e.g., X-CH_2O and X-CH_3OOH) having the same chemical production and destruction terms, except in the upper troposphere (above about 6 km), where their chemical production is set to zero. Their concentrations in the upper troposphere therefore represent the contribution of their injection from the lower troposphere. Note that this formulation is not exactly equivalent to calculating the impact of deep convection, because transport by the synoptic winds is also included and convective downdrafts are not taken into account.

Finally, the photooxidation of acetone, initiated by

$$CH_3COCH_3 + h\nu\ (+O_2) \rightarrow CH_3CO_3 + CH_3O_2 \quad (16)$$
$$CH_3COCH_3 + OH\ (+O_2) \rightarrow CH_3COCH_2O_2 + H_2O \quad (17)$$

is a particular but important source of HO_x. Because of its photochemical lifetime of several weeks, acetone is present in the upper troposphere at relatively high concentrations, of the order of 500 pptv [*Singh et al.*, 1995]. Both the reaction with OH (reaction (17)) and photolysis (reaction (16)) are important sinks globally, but photolysis is by far dominant above about 10 km altitude. The net HO_x yield for photolysis (followed by reactions (3)-(10) and (12)-(15)) peaks at the tropopause (about 100 mbar in the tropics and 200 mbar at midlatitudes during the summer), with values of about 3. The OH reaction (17), followed by a series of reactions leading eventually to species like CH_3CO_3, CH_2O, and HO_2 [see, e.g., *Singh et al.*, 1995], is a HO_x source in most regions, with a yield exceeding 2 around the tropopause region.

Other primary sources play a minor role in the upper troposphere, for example, the oxidation of methane and H_2 initiated by their reaction with $O(^1D)$ and the photolysis of nitric acid and PAN formed in the lower troposphere. We verified, however, that their contributions are always small (at most a few percent of the total) in the troposphere.

4. Results

The zonally averaged relative contributions of the different sources to the total primary source of HO_x are displayed in Figures 5 (January) and 6 (July). The total primary production is shown in Figure 7 for the month of July. As expected, the lowest values of HO_x production are predicted at the tropopause and in the winter midlatitudes and high latitudes. It should be remembered that significant departures from these average ("climatological") contributions can occur episodically at the regional scale, for example, following a strong convective event. Note that here the total source excludes the secondary sources, since the role of these processes is to amplify the primary sources. The amplification of the total primary source (increase in percent) due to CH_4+OH (not shown) is found to be significant near the tropopause, with values ranging between 30 and about 80% (at high latitudes around 200 mbar). The predominantly low-NO_x conditions prevailing in the middle troposphere (up to about 7 km altitude) result in a net HO_x sink due to CH_4+OH in this region, owing to reactions (4)-(6). The

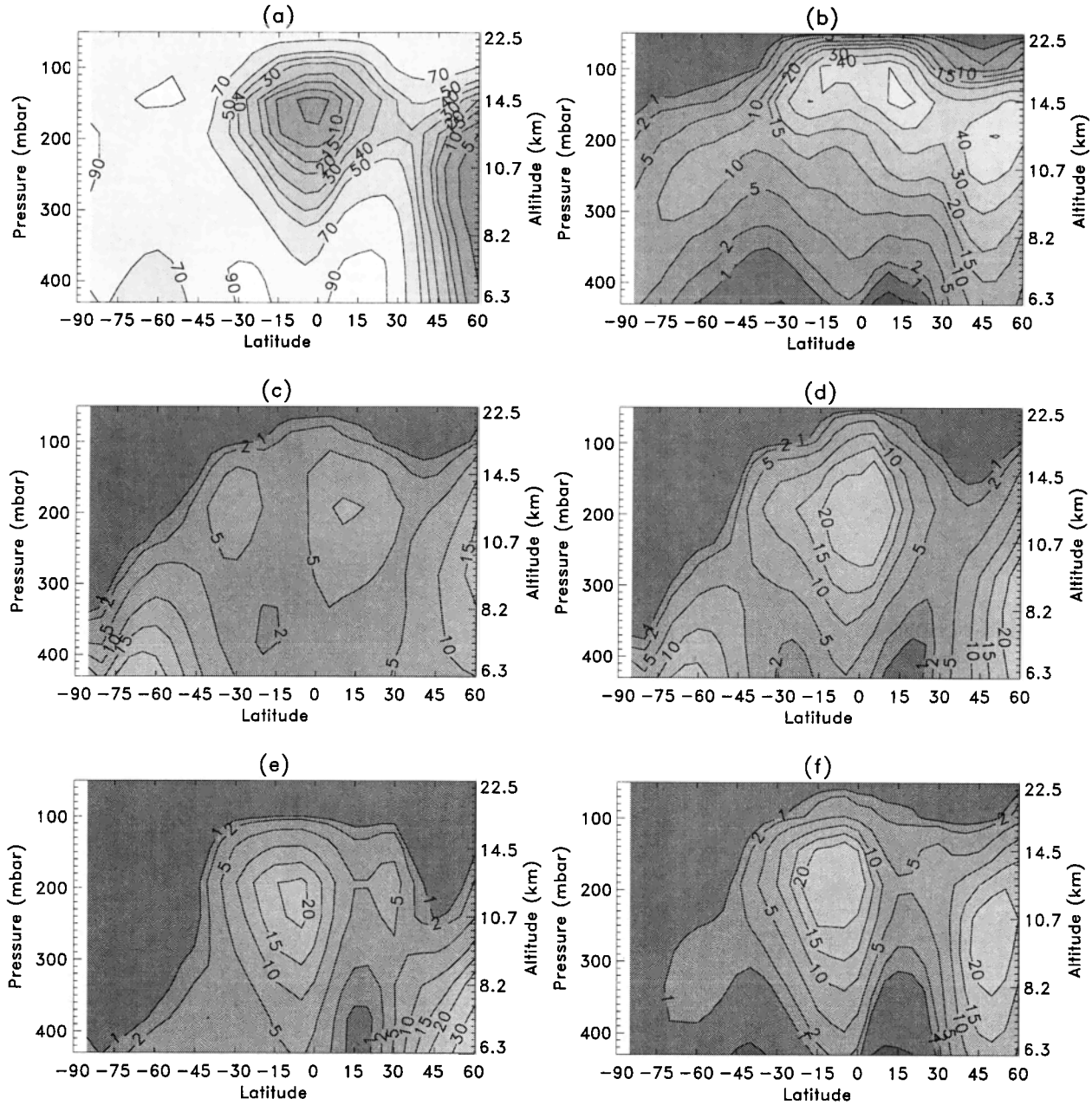

Figure 5. Calculated relative contributions (zonal means in percent) of (a) O_3 photolysis, (b) acetone photooxidation, (c) photolysis of lower tropospheric H_2O_2, (d) photooxidation of lower tropospheric CH_3OOH, (e) photolysis of lower tropospheric CH_2O, and (f) photooxidation of C_2 aldehydes, to the total primary source of HO_x in the upper troposphere in January. See text for details. Contours are 1, 2, 5, 10, 15, 20, 30, 40, 50, 70, and 90%.

impact of ethane's oxidation by OH has similar features but is more than 1 order of magnitude smaller than the impact of methane oxidation.

As can be seen in Figures 5a and 6a, ozone photolysis (followed by $O(^1D)+H_2O$) is dominant (>70%) in the middle troposphere and to a somewhat lesser extent in the summertime midlatitudes upper troposphere. In the tropical upper troposphere, as well as in the wintertime midlatitudes, however, the contribution of ozone photolysis to the total source of HO_x drops to below 50% and down to only a few percent at some locations. Since we have seen that the model tends to overestimate ozone in the 20°-35°N region, the calculated contribution of ozone photolysis shown in Figures 5 and 6 should be regarded as a high estimate in these areas. The contribution of acetone photooxidation (mostly photolysis) is predicted to be largest at and just below the tropopause, in accord with previous results based on observations, such as the Stratospheric Tracers of Atmospheric Transport (STRAT) campaign [*Jaeglé et al.*, 1997]. The diurnally and zonally averaged contribution of acetone photooxidation reaches about 30-50% in the tropics (between 100 and 150 mbar) and between 20% (July) and about 40% (January) at the northern midlatitudes, in particular, in the civil aircraft corridors (10-11 km altitude, 40°-60°N). The "convective" sources (Figures 5c-5f and Figures 6c-6f) are maximum in the upper troposphere at generally

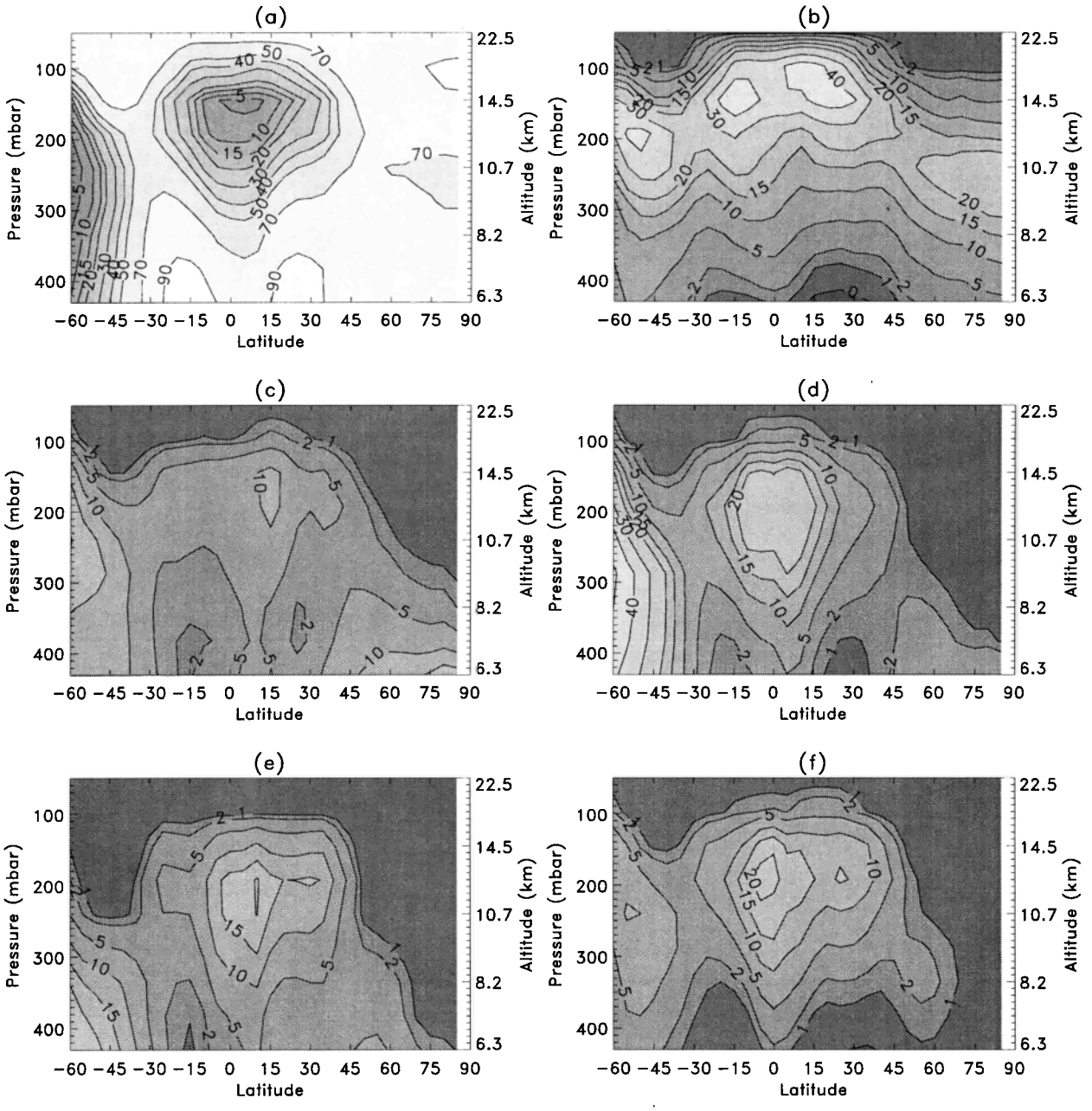

Figure 6. Same as Figure 5 but for the month of July.

lower altitudes, mostly because their short photochemical lifetimes do not allow them to be transported much higher than the convective injection altitude. Around 200 mbar in the tropics and around 300 mbar in the wintertime midlatitudes, these sources are found to be dominant. The convective injection of H_2O_2 is found to be the least significant HO_x source, despite the relatively large H_2O_2 mixing ratios in the boundary layer (see Figure 3). This results from the assumed efficient rainout of H_2O_2 in the convective updrafts. Note that here the solubility of CH_3OOH and the aldehydes was assumed to be too low to significantly reduce the amount of these gases when transported to the upper troposphere. This assumption should be valid for the weakly soluble CH_3OOH but can lead to some overestimation of the aldehydes' contribution shown here. The photooxidation of lower tropospheric CH_3OOH, CH_2O, and C_2 aldehydes is seen to be of similar magnitude (up to about 25% each) when zonally averaged. However, their geographical distribution (displayed in Figure 8, 240 mbar level in July) shows important differences. The convective injection of CH_3OOH is seen to be dominant over the tropical oceans, in agreement with previous estimates [*Prather and Jacob*, 1997]. The impact of the H_2O_2 photolysis reaches high values at some locations in the tropics (see Figure 8c), where, with the parameterization used in the model, the large vertical wind shear induces a low convective precipitation efficiency. Despite the fact that the boundary layer concentrations of CH_3OOH are only slightly higher over the oceans than over the continents, and that H_2O_2 is often most abundant over the continents, the role of the peroxides is seen to be almost negligible over continents, where the aldehydes (and to a lesser extent acetone) are found to be dominant. The concentrations of aldehydes (several parts per

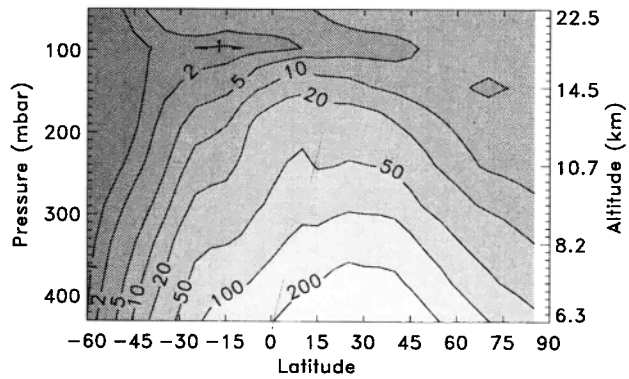

Figure 7. Calculated primary production of HO_x (zonal mean) in the upper troposphere in July (10^3 molecules per cm^{-3} s^{-1}).

billion by volume near the NMHC emission areas) greatly exceed that of peroxides in the continental boundary layer.

5. Relevance to Ozone Photochemical Production

In order to estimate the significance of these results with respect to ozone photochemical production and issues such as the impact of aircraft NO_x emissions, let us first write the net ozone production as $P - L$, where P and L are the photochemical production and loss terms, and $P=P_1+P_2+P_3$, where P_1 is the production of odd oxygen (O_x) due to the HO_2+NO reaction, P_2 is the production by CH_3O_2+NO associated with the methane oxidation by OH, and P_3 is the sum of the other terms, i.e., ozone production due to O_2 photolysis in the stratosphere and NMHC degradation (through RO_2+NO reactions) in the troposphere. Both P_1 and P_2 are proportional to HO_x concentrations. We calculate

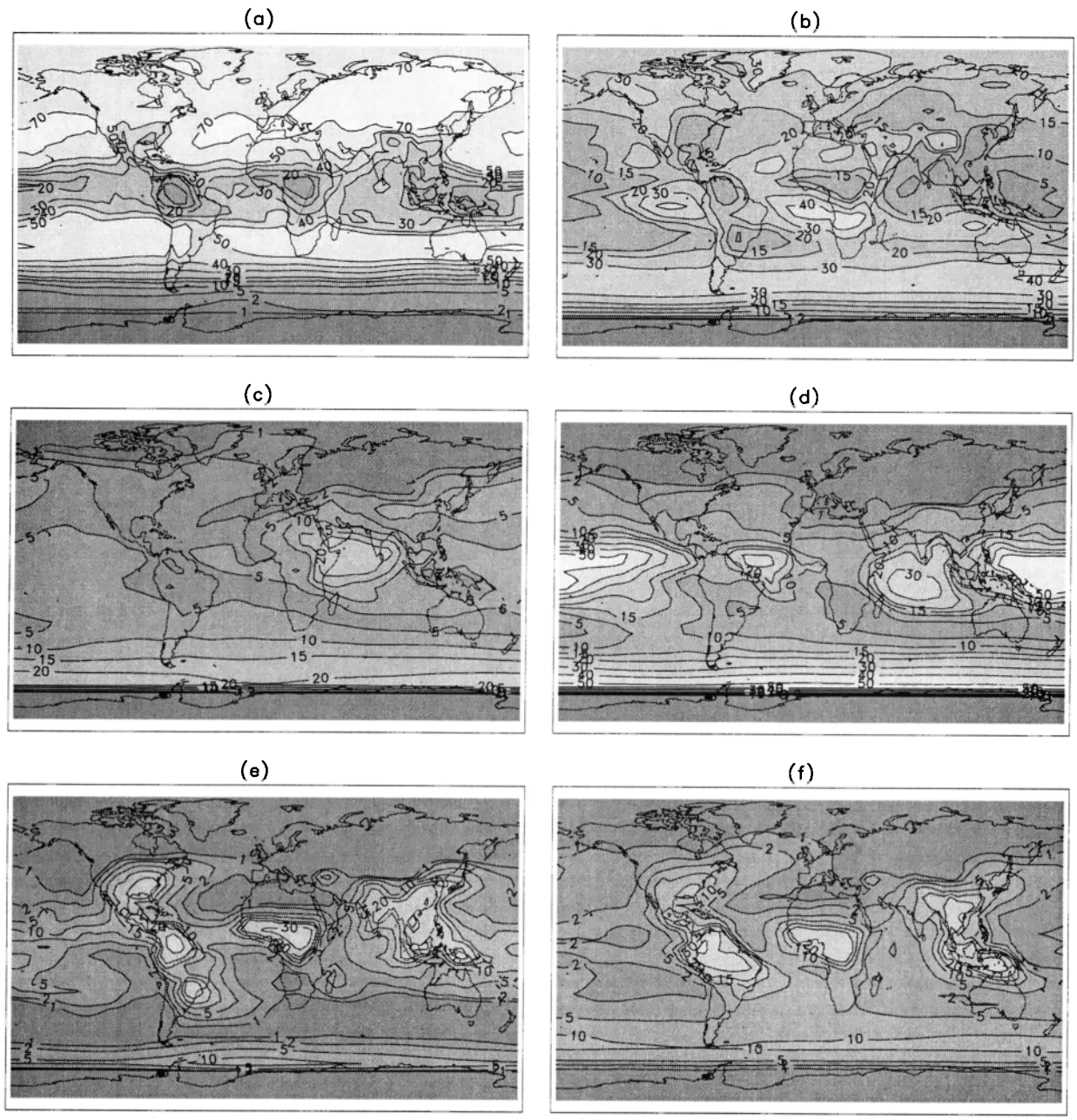

Figure 8. As in Figure 6 but at the 240 mbar level (July).

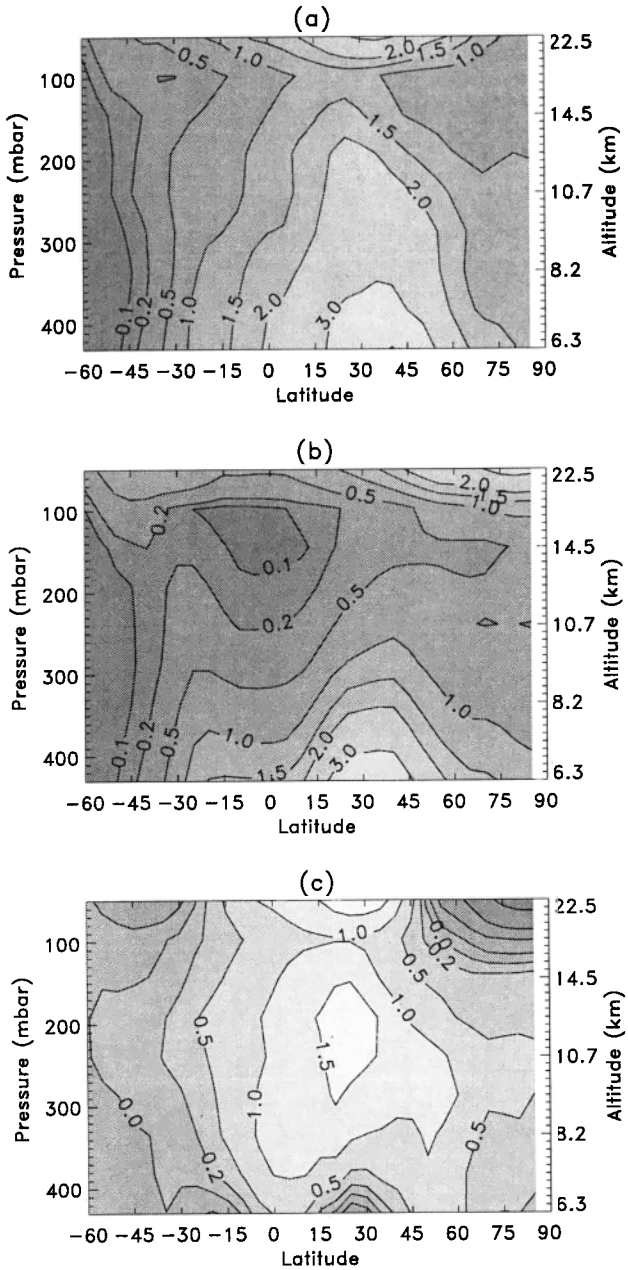

Figure 9. Calculated photochemical (a) production,(b) loss, and (c) net production of ozone (10^5 molecules per cm^{-3} s^{-1}) in the upper troposphere in July (zonal averages).

that while HO_2+NO represents about 50% of the total ozone production in the boundary layer, its importance increases to more than about 80% in the upper troposphere, because of the lower NMHC abundances and the slower rate of methane oxidation at these altitudes. The sum P_1+P_2 amounts to 85-95% of the total ozone production in the upper troposphere. In other words, ozone production is almost proportional to HO_x levels. Figure 9 displays the model-calculated P, L, and P - L terms (zonal average for July). A striking feature is the low destruction rate in the upper troposphere, compared to ozone production, especially in the tropics. Ozone production is typically between 2 and 10 times as large as ozone loss, so that the net production of ozone is almost always positive and often quite close to ozone production. This is mostly due to the low water vapor mixing ratios (causing the $O(^1D)$+H_2O sink to be small) and cold temperatures (favoring HO_2+NO compared to HO_2+O_3 and NO+O_3, owing to their temperature dependence) typical of the upper troposphere. We conclude that any process leading to a HO_x level increase in the upper troposphere will generally increase ozone net production in a roughly linear way, as least insofar as the chemical feedbacks (see next paragraph) can be ignored. This is, however, not true everywhere: for example, NO_x is too low for net ozone production in large areas of the Pacific Ocean according to the model calculations, in agreement with the conclusions of *Folkins et al.* [1998] based on an analysis of the PEM-West B campaign. It follows that the convective injection of peroxides (CH_3OOH in particular), important over tropical oceans, will be generally much less efficient in producing ozone than the other sources.

Even in high-NO_x regions, however, ozone production increases less than linearly with an increase in the HO_x sources. First, the main HO_x sinks in the upper troposphere (OH+HO_2, H_2O_2 formation and removal, and OH+HNO_4) are largely quadratic in HO_x, so that the change in HO_x concentration will be closer to the square root of the HO_x source change, if the OH/HO_2 ratio remains unchanged. Second, the processes that change the HO_x source also modify the NO_x budget, for example, through OH+NO_2 or, in the case of NMHC oxidation, through increased PAN formation. In all cases, NO_x levels are decreased, and ozone formation (if not the ozone production efficiency per unit NO_x) is dampened.

In order to illustrate the impact of HO_x sources on ozone, the model has been used to investigate the impact of acetone on the HO_x, NO_x, and ozone budgets. Figure 10 shows the zonally averaged changes in HO_2, OH, NO concentrations, and ozone production resulting from the inclusion of acetone in the model. The concentrations of HO_2 and OH increase when acetone is included in the model, with a distribution consistent with the contribution of acetone to the primary HO_x sources (Figure 6b). The NO_x levels are decreased by about 10-16%, mainly because of increased PAN formation. The PAN levels are increased by about 20-60% in the same regions. The decreased NO_x results in a lower OH/HO_2 ratio, therefore inhibiting the quadratic HO_x sink increase associated with OH+HO_2 and OH+HNO_4. In the aircraft flight corridors, in particular (10 km altitude at midlatitudes), OH changes are small, and the percent increase in HO_2 (roughly equal to the change in HO_x) is almost equal to the calculated contribution of acetone to the primary source of HO_x. Other effects (e.g., decreased role of OH+NO_y reactions due to the lower NO_x levels and repartitioning of NO_y as a result of HO_x changes) might explain why the HO_2 level changes in the tropical upper troposphere are only slightly lower than the contribution of acetone to the total HO_x source. Ozone production increases by about 10% in the flight corridors, reflecting primarily the changes in HO_2 and NO.

Figure 11 displays the calculated impact of the current aircraft emissions on zonally averaged ozone levels in July, without and with acetone in the model. A maximum change of about 5% is predicted at the flight altitude, comparable to previous estimates [e.g., *Brasseur et al.*, 1996; *Friedl*, 1997]. Including acetone in the model is calculated to increase the aircraft impact by about 20%, similar to the change in HO_x level due to acetone at this location.

6. Conclusions

A three-dimensional chemical-transport model of the troposphere has been used to quantify the magnitude of the major HO_x sources in the upper troposphere. Although $O(^1D)$+H_2O is the

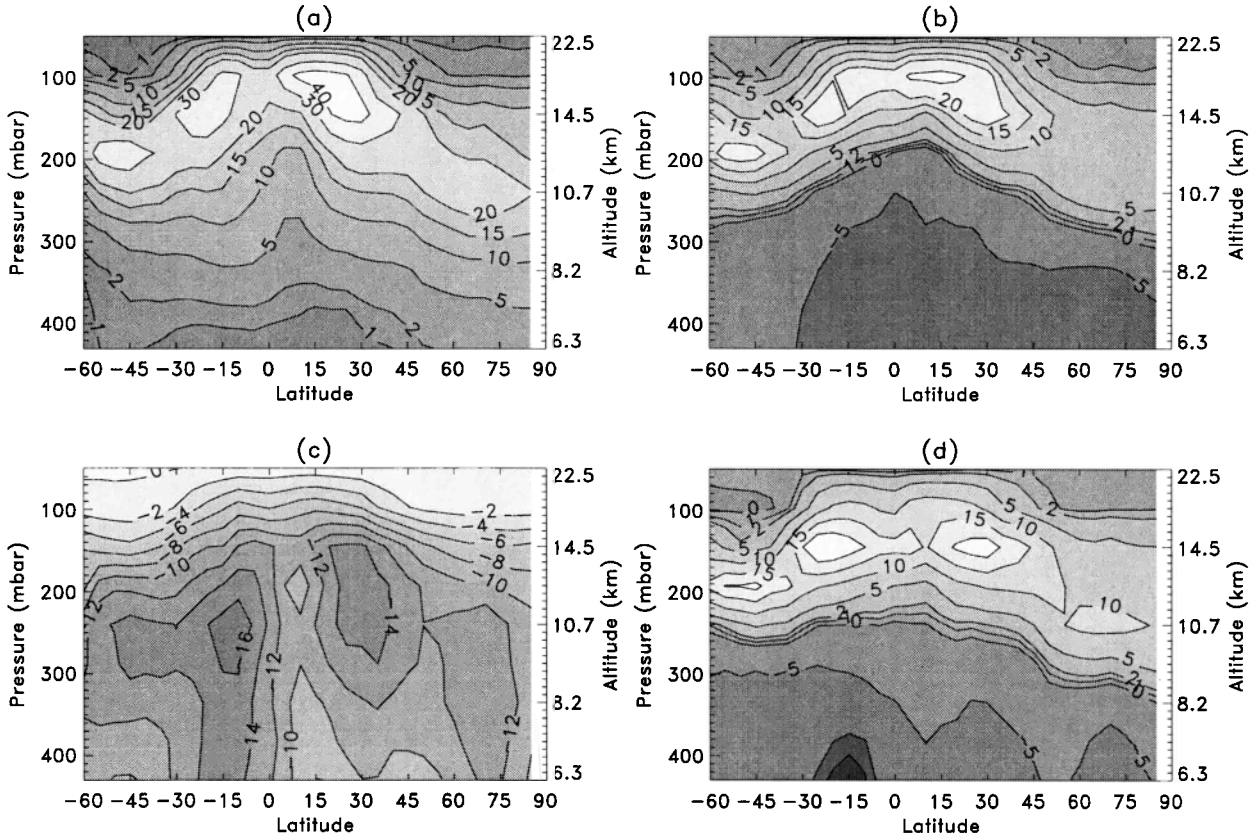

Figure 10. Calculated changes (in percent) in (a) HO_2, (b) OH, (c) NO levels, and (d) ozone production associated with the inclusion of acetone in the calculations (July).

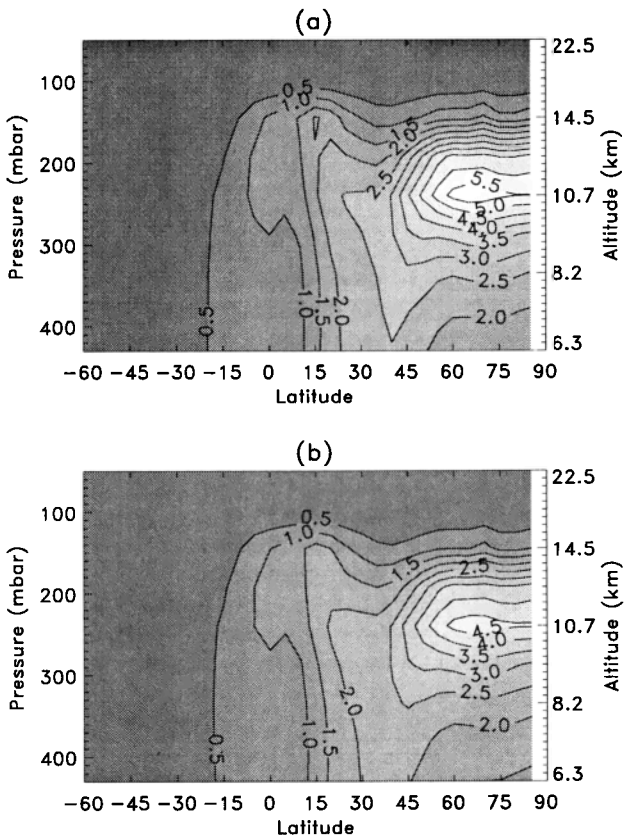

Figure 11. Calculated impact of current (1992) aircraft emissions of NO_x on zonally averaged ozone mixing ratios (July) (a) with acetone and (b) without acetone.

major source in most of the troposphere, other processes are shown to play an important role in the upper troposphere, in particular, in the tropics and in the wintertime midlatitudes. In the tropopause region, acetone photolysis represents typically 20-40% of the total primary source of HO_x. At slightly lower altitudes the convective injection of peroxides (mostly over oceanic areas) and aldehydes (over continents) adds up to 50% or more of the total HO_x in the tropics and the wintertime upper troposphere. Although the relationship between HO_x production and ozone production is complex because of the chemical feedbacks involving HO_x and NO_x species, ozone net production generally increases with the HO_x source in the upper troposphere. The model calculations suggest that acetone photooxidation contributes to about 20% of the HO_x primary source in the aircraft flight corridors in July. Including acetone in model calculations results in a 20% higher HO_x level, as well as a 20% higher ozone production efficiency per unit NO_x in the same region.

The calculations presented here suffer from important uncertainties. In particular, the coupling between washout and vertical transport in convective updrafts for soluble species such as hydrogen peroxide and formaldehyde requires further investigations. Although the budget of acetone used in the model calculations leads to modeled atmospheric concentrations that agree relatively well with the observations, the individual acetone sources are not well characterized. Finally, the large importance of other nonmethane hydrocarbons (e.g., C_2 aldehydes) in our results suggests that improved chemical mechanisms for NMHC degradation are essential, even for the supposedly remote upper troposphere.

Acknowledgments. We thank L. Horowitz and E. Atlas for their thoughtful comments. This work has been made possible by a grant of the Belgian Office for Scientific, Technological and Cultural Affairs (OSTC).

The National Center for Atmospheric Research is operated by the University Corporation for Atmospheric Research under sponsorship of the National Science Foundation.

References

Andreae, M. O., et al., Methyl halide emissions from savanna fires in southern Africa, *J. Geophys. Res.*, *101*, 23,585-23,595, 1996.

Arlander, D. W., D Brüning, U. Schmidt, and D. Ehhalt, The tropospheric distribution of formaldehyde during TROPOZ II, *J. Atmos. Chem*, *22*, 251-268, 1995.

Arnold, F, V. Burger, B. Droste-Frank, F Grimm, A. Krieger, J Schneider, and T. Stilp, Acetone in the upper troposphere and lower stratosphere: Impact on trace gases and aerosols, *Geophys. Res Lett.*, *24*, 3017-3020, 1997.

Balkanski, Y. J., D. J. Jacob, G. M Gardner, W. C Graustein, and K K Turekian, Transport and residence times of continental aerosols inferred from a global three-dimensional simulation of ^{210}Pb, *J Geophys Res.*, *98*, 20,573-20,586, 1993.

Benkovitz, C. M., J. Dignon, J. Pacyna, T. Scholtz, L. Tarrason, E. Voldner, and T E. Graedel, Global inventories of anthropogenic emissions of SO_2 and NO_x, *J. Geophys Res.*, *101*, 29, 239-29,250, 1996.

Brasseur, G., J.-F. Müller, and C. Granier, Atmospheric impact of NO_x emissions by subsonic aircraft: A three-dimensional study, *J Geophys. Res*, *101*, 1423-1428, 1996.

Brocard, D., J.-P Lacaux, and H. Eva, Domestic biomass combustion and associated atmospheric emissions in West Africa, *Global Biogeochem Cycles*, *12*, 127-139, 1998.

Chatfield, R B , and P. J. Crutzen, Sulfur dioxide in remote oceanic air: Cloud transport of reactive precursors, *J. Geophys. Res.*, *89*, 7111-7132, 1984

Costen, R.C., G.M. Tennille, and J.S. Levine, Cloud pumping in a one-dimensional model, *J. Geophys. Res.*, *93*, 15,941-15,954, 1988.

De More, W. B , S. P Sander, D. M. Golden, R. F Hampson, M. J. Kurylo, C J. Howard, A. R. Ravishankara, C. E. Kolb, and M J Molina, Chemical kinetics and photochemical data for use in stratospheric modeling, *JPL Publ., 97-4*, 1997.

Dentener, F. J., and P. J. Crutzen, A three-dimensional model of the global ammonia cycle, *J. Atmos. Chem.*, *19*, 331-369, 1994.

Folkins, I., P O. Wennberg, T. F. Hanisco, J. G Anderson, and R J Salawitch, OH, HO_2, and NO in two biomass burning plumes: Sources of HO_x and implications for ozone production, *Geophys. Res. Lett.*, *24*, 3185-3188, 1997.

Folkins, I., R. Chatfield, H. Singh, Y. Chen, and B. Heikes, Ozone production efficiencies of acetone and peroxides in the upper troposphere, *Geophys. Res. Lett., 25*, 1305-1308, 1998.

Friedl, R. R. (Ed.), Atmospheric effects of subsonic aircraft: Interim assessment report of the advanced subsonic technology program, *NASA Ref. Publ. 1400*, 168 pp., 1997.

Fritsch, J. M., and C. F. Chappell, Numerical prediction of convectively driven mesoscale systems, 1. Convective parameterization, *J. Atmos Sci.*, *37*, 1722-1733, 1980.

Granier, C., W M Hao, G. Brasseur, and J.-F. Müller, Land use practices and biomass burning: Impact on the chemical composition of the atmosphere, in *Biomass Burning and Global Change*, edited by J. S. Levine, pp. 140-148, MIT Press, Cambridge, Mass., 1996.

Guenther, A., et al , A global model of natural volatile organic compound emissions, *J. Geophys. Res.*, *100*, 8873-8892, 1995.

Hauglustaine, D., G Brasseur, S. Walters, P. J. Rasch, J.-F. Müller, L. K. Emmons, and M. A. Carroll, MOZART. A global chemical transport model for ozone and related chemical tracers, 2, Model results and evaluation, *J Geophys. Res.*, in press, 1998.

Jaeglé, L , et al., Observed OH and HO_2 in the upper troposphere suggest a major source from convective injection of peroxides, *Geophys. Res. Lett.*, *24*, 3181-3184, 1997.

Jenkin, M E., S. M. Saunders, and M. J. Pilling, The tropospheric degradation of volatile organic compounds: A protocol for mechanism development, *Atmos Environ*, *31*, 81-104, 1997.

Kanakidou, M., H. B Singh, K. M. Valentin, and P. J. Crutzen, A two-dimensional study of ethane and propane oxidation in the troposphere, *J. Geophys. Res.*, *96*, 15,395-15,413, 1991.

Levy, H., II, Photochemistry of the lower troposphere, *Planet Space Sci.*, *20*, 919-935, 1972.

Logan, J A., M J Prather, S. C. Wofsy, and M B McElroy, Tropospheric chemistry: A global perspective, *J. Geophys Res*, *86*, 7210-7254, 1981.

McKeen, S. A., T. Gierczak, J. B. Burkholder, P. O. Wennberg, T. Hanisco, E. R Keim, R.-S Gao, S. C. Liu, A. R. Ravishankara, and D. W Fahey, The photochemistry of acetone in the upper troposphere. A source of odd-hydrogen radicals, *Geophys. Res. Lett.*, *24*, 3177-3180, 1997.

Muller, J -F., and G. Brasseur, IMAGES. A three-dimensional chemical transport model of the global troposphere, *J. Geophys. Res.*, *100*, 16,445-16,490, 1995.

Pickering, K. E , Y. Wang, W.-K. Tao, C. Price, and J.-F. Müller, Vertical distributions of lightning NO_x for use in regional and global chemical transport models, *J Geophys. Res.*, in press, 1998.

Prather, M. J., and D. J. Jacob, A persistent imbalance in HO_x and NO_x photochemistry of the upper troposphere driven by deep tropical convection, *Geophys. Res Lett*, *24*, 3189-3192, 1997.

Price, C., J Penner, and M. Prather, NO_x from lightning, 1, Global distribution based on lightning physics, *J. Geophys. Res.*, *102*, 5929-5941, 1997

Singh, H. B , M Kanakidou, P. J. Crutzen, and D J. Jacob, High concentrations and photochemical fate of oxygenated hydrocarbons in the global troposphere, *Nature*, *378*, 50-54, 1995.

Slemr, F., and H. G Tremmel, Hydroperoxides in the marine troposphere over the Atlantic Ocean, *J Atmos. Chem.*, *19*, 371-404, 1994.

Wang, Y., D. J. Jacob, J A Logan, and C. M. Spivakovsky, Global simulation of tropospheric O_3-NO_x-hydrocarbon chemistry, 1, Model formulation, *J. Geophys. Res.*, *103*, 10,713-10,725, 1998a.

Wang, Y , J. A Logan, D. J. Jacob, and C. M. Spivakovsky, Global simulation of tropospheric O_3-NO_x-hydrocarbon chemistry, 2, Model evaluation and global ozone budget, *J. Geophys. Res.*, *103*, 10,727-10,755, 1998b

Wennberg, P., et al., Hydrogen radicals, nitrogen radicals, and the production of ozone in the middle and upper troposphere, *Science*, *279*, 49-53, 1998

Yienger, J. J., and H Levy II, Empirical model of global soil-biogenic NO_x emissions, *J. Geophys. Res.*, *100*, 11,447-11,464, 1995.

G. Brasseur, National Center for Atmospheric Research, P O Box 3000, Boulder, CO 80303

J.-F. Müller, Belgian Institute for Space Aeronomy, Ave circulaire 3, Brussels, Belgium B-1180. (e-mail: jfm@oma.be)

(Received June 3, 1998; revised August 28, 1998; accepted August 31, 1998.)